View metadata, citation and similar papers at core.ac.uk

brought to you by CORE

provided by Warwick Research Archives Portal Repository

Original citation:
Prindle, Arthur, Liu, Jintao, Asally, Munehiro , Ly, San, Garcia-Ojalvo, Jordi and Süel, Gürol M.. (2015) Ion channels enable electrical communication in bacterial communities. Nature.
Permanent WRAP url:
http://wrap.warwick.ac.uk/73527

Copyright and reuse:
The Warwick Research Archive Portal (WRAP) makes this work of researchers of the University of Warwick available open access under the following conditions. Copyright © and all moral rights to the version of the paper presented here belong to the individual author(s) and/or other copyright owners. To the extent reasonable and practicable the material made available in WRAP has been checked for eligibility before being made available.

Copies of full items can be used for personal research or study, educational, or not-for-profit purposes without prior permission or charge. Provided that the authors, title and full bibliographic details are credited, a hyperlink and/or URL is given for the original metadata page and the content is not changed in any way.
Publisher statement:
http://dx.doi.org/10.1038/nature15709

A note on versions:
The version presented here may differ from the published version or, version of record, if you wish to cite this item you are advised to consult the publisher's version. Please see the 'permanent WRAP url' above for details on accessing the published version and note that access may require a subscription.

For more information, please contact the WRAP Team at: publications@warwick.ac.uk

warwickpublicationswrap

highlight your research

http://wrap.warwick.ac.uk/

Ion channels enable electrical communication within bacterial communities

Arthur Prindle[1], Jintao Liu[1]*, Munehiro Asally[2]*, San Ly[1], Jordi Garcia-Ojalvo[3], Gürol M. Süel[1#]

[1] Division of Biological Sciences, University of California San Diego, California 92093, USA

[2] Warwick Integrative Synthetic Biology Centre, School of Life Sciences, University of Warwick, Coventry CV4 7AL, UK

[3] Department of Experimental and Health Sciences, Universitat Pompeu Fabra, 08003 Barcelona, Spain

* These authors contributed equally to this work.

Corresponding author: gsuel@ucsd.edu

Abstract

The study of bacterial ion channels has provided fundamental insights into the structural basis of neuronal signaling. However, the native role of ion channels in bacteria has remained elusive. Here we show that ion channels conduct long-range electrical signals within bacterial biofilm communities through spatially propagating waves of potassium. These waves result from a positive feedback loop, in which a metabolic trigger induces release of intracellular potassium, which in turn depolarizes neighboring cells. Propagating through the biofilm, this wave of depolarization coordinates metabolic states among cells in the interior and periphery of the biofilm. Deletion of the potassium channel abolishes this response. As predicted by a mathematical model, we further show that spatial propagation can be hindered by specific genetic perturbations to potassium channel gating. Together, these results demonstrate a function for ion channels in bacterial biofilms, and provide a prokaryotic paradigm for active, long-range electrical signaling in cellular communities.

Introduction

Communication through electrical signaling is prevalent among biological systems. One of the most familiar examples is the action potential in neurons that is mediated by ion channels. For many years, the study of bacterial ion channels has provided fundamental insights into the structural basis of such neuronal signaling[1,2]. In particular, the prokaryotic potassium ion channel KcsA provided the first structural information on ion selectivity and conductance[3]. More recently, it has been shown that bacteria possess many important classes of other ion channels such as sodium channels[4], chloride channels[5], calcium-gated potassium channels[6] and ionotropic glutamate receptors[7] similar to those found in neurons. However, the native role of these ion channels in bacteria has largely remained

unclear[8,9]. Pioneering efforts to uncover ion channel function in bacteria have identified roles in the extreme acid resistance response[5] and in osmoregulation[10], yet ion-specific channels do not appear to be solely responsible for these cellular processes. It thus remains unclear whether ion channels can support other unique functions in prokaryotes. We hypothesized that studying bacteria in their native context, the biofilm community, may reveal new clues about the function of ion channels in bacteria.

Bacterial biofilms are organized communities containing billions of densely packed cells. Such communities can exhibit fascinating macroscopic spatial coordination[11–16]. However, it remains unclear how microscopic bacteria could communicate effectively over large distances. To investigate this question, we studied a *Bacillus subtilis* microbial community that was recently reported to undergo metabolic oscillations triggered by nutrient limitation[17]. The oscillatory dynamics resulted from long-range metabolic codependence between cells in the interior and periphery of the biofilm (Figure 1a)[17]. Specifically, interior and peripheral cells compete for glutamate, while sharing ammonium. As a result, biofilm growth halts periodically, increasing nutrient availability for the sheltered interior cells. Interestingly, glutamate (Glu^-) and ammonium (NH_4^+) are both charged metabolites, whose respective uptake and retention is known to depend on the transmembrane electrical potential and proton motive force (PMF)[18,19]. Therefore, we wondered whether metabolic coordination among distant cells within the biofilm might also involve a form of electrochemical signaling.

Oscillations in membrane potential

In order to monitor long-range electrical fluctuations in the bacterial community as a function of space and time, we grew biofilms in an unconventionally large microfluidic device (Figure 1b and Supplementary Information: Microfluidics). To measure electrical signaling, we used the fluorescent

cationic dye Thioflavin T (ThT) to quantify membrane potential within the biofilm. ThT is positively charged and can be retained in cells because of their inside-negative electrical membrane potential. Thus, cells with a negative membrane potential will retain more ThT, allowing it to act as a Nernstian voltage indicator[20,21]. We confirmed that ThT faithfully reports the membrane potential by comparing it to $DiSC_3(5)$, an established reporter of membrane potential in bacteria (Extended Data Figure 1a)[22]. We find that ThT has an approximately three fold higher sensitivity to changes in membrane potential compared to $DiSC_3(5)$ (Extended Data Figure 1a, inset). Furthermore, we exposed cells to minor changes in external pH, which is known to alter membrane potential[23], and indeed observed the expected changes in ThT (Extended Data Figure 1b). Therefore, ThT accurately reports on changes in membrane potential for bacteria residing in biofilms.

We next investigated changes in membrane potential during metabolic oscillations. In particular, quantitative measurements of ThT fluorescence showed global and self-sustained oscillations consistent with the reported period of the metabolic oscillations (Figure 1c, Supplementary Video 1 and Extended Data Figure 1c)[17]. Furthermore, oscillations in ThT could be quenched by supplementation of the media with glutamine, which bypasses the need for glutamate and ammonium (Extended Data Figure 1d). These data show a connection between metabolic oscillations and membrane potential. Strikingly, oscillations in membrane potential were synchronized among even the most distant regions of the biofilm community (Figure 1d,e). We wondered whether active electrochemical signaling could be responsible for this long-range synchronization.

Active propagation of potassium signal

Changes in membrane potential involve the movement of charged species across the cellular membrane. We suspected potassium, since it is the most abundant cation in all living cells[24] and has

been implicated to play a role in biofilm formation[25,26]. *B. subtilis* uses active potassium transport mechanisms to concentrate intracellular potassium at approximately 300 mM[27–29]. This intracellular concentration is nearly 40 times the external media concentration. Consequently, sudden release of this potassium gradient would increase extracellular potassium concentration and generate a change in the membrane potential. Accordingly, we used a fluorescent chemical potassium dye, Asante Potassium Green-4 (APG-4[30]), to measure the extracellular concentration of potassium in the biofilm (Figure 2a and Extended Data Figure 2a,b). We observed global oscillations in APG-4 that correlated with membrane potential, which suggests that the membrane potential oscillations could involve the release of potassium (Figure 2b,c and Supplementary Video 2). In agreement with this finding, oscillations in extracellular potassium extended beyond the biofilm to flood the surrounding growth media (Extended Data Figure 2c). We also measured the dynamics of sodium, another ion commonly utilized by cells to modulate membrane potential, and observed no oscillations (Extended Data Figure 2d-f). Together, these data suggest that potassium plays a role in the synchronized oscillations in membrane potential.

Furthermore, we directly tested that oscillations in membrane potential were driven by flow of potassium across the cell membrane. Specifically, we clamped net potassium flux across the cell membrane by supplementing the growth media with 300 mM KCl (matching the intracellular K concentration) (Figure 2d). When we applied this chemical potassium clamp, oscillations in membrane potential abruptly halted (Figure 2e). Applying this clamp together with valinomycin, a potassium ionophore that acts as potassium-specific carrier in the cellular membrane[31], yielded a similar quenching of oscillations (Extended Data Figure 3a,b). Therefore, changes in the electrochemical potential for potassium appear to be required for the observed oscillations in membrane potential.

Next, we determined whether cells could actively propagate the extracellular potassium signal through the biofilm to sustain long-range communication. While diffusive signals decay over space and time, active signaling processes can amplify the signal avoiding such decay (Figure 2f). To discriminate which of these processes may be operating in the biofilm, we observed the propagation of the extracellular potassium signal (Figure 2g). Results show that the signal travels at a constant rate of propagation (Extended Data Figure 3c,d). Furthermore, the amplitude of the signal does not decay with distance traveled, in contrast to what is predicted for passive potassium diffusion (Figure 2h). These findings are consistent with a process in which cells actively propagate the potassium signal. Together, these results suggest that the biofilm synchronizes global oscillations in membrane potential by an active signaling process involving potassium ions.

Potassium ion channel-mediated signaling

Motivated by our findings, we explored the role of ion channels in the observed potassium signaling. We focused on YugO, the only experimentally described potassium channel in *B. subtilis*, which is also reported to be important for biofilm formation[32]. Potassium flux through YugO is gated by an intracellular TrkA domain, known to be regulated by the metabolic state of the cell[33–35]. Accordingly, we hypothesized that metabolic limitation could form the initial trigger for YugO activation. Specifically, since glutamate limitation is known to drive the underlying metabolic oscillations[17], we anticipated that transient removal of glutamate should initiate potassium release. To test this, we transiently deprived cells of glutamate and measured extracellular potassium in both wild type and *yugO* deletion strains (Supplementary Information: Strains). As expected, we observed extracellular potassium release from wild-type, but not the *yugO* deletion strain (Figure 3a). These findings indicate that glutamate limitation can trigger the potassium signal by activating the YugO potassium channel.

Next, we investigated whether YugO also plays a role in the active propagation of the potassium signal. To test this, we measured the response of wild-type and *yugO* deletion strains to transient bursts of external potassium (300 mM KCl). As expected, potassium exposure first resulted in a short-term membrane potential depolarization in both strains. However, in the wild-type this initial depolarization was followed by hyperpolarization, which was not observed in the *yugO* deletion strain (Figure 3b). This period of hyperpolarization was accompanied by an increase in extracellular potassium (Extended Data Figure 4a). Together, these data indicate that potassium exposure triggers a release of intracellular potassium through YugO. Exposure to an equivalent concentration of sorbitol (an uncharged solute) did not elicit a response, ruling out osmotic effects (Extended Data Figure 4b). Therefore, YugO appears to play a role in propagating the extracellular potassium signal within the biofilm.

Mathematical modeling of electrical signaling

Our data thus points to a mechanism where metabolically stressed cells release intracellular potassium, and the resulting elevated extracellular potassium imposes further metabolic stress onto neighboring cells (Figure 3c). In *B. subtilis,* glutamate is co-transported with 2 protons by the GltP transporter and this process depends on the proton motive force (PMF)[18]. Potassium mediated depolarization of the membrane potential can transiently reduce the electrical component of the PMF[23], and thereby lower glutamate uptake and intracellular ammonium retention[18,19]. Therefore, potassium mediated signaling could propagate metabolic stress onto distant cells (Figure 3c, right). Accordingly, hyperpolarization triggered by YugO activation may represent a cellular response to enhance glutamate uptake or ammonium retention. This notion is supported by our finding that the response to extracellular potassium can be abolished by growing cells in glutamine, an uncharged metabolite and preferred nitrogen source that bypasses the need for glutamate and ammonium[36]

(Extended Data Figure 4c). This result further supports the specific link between potassium mediated electrical signaling and metabolic stress.

To determine whether the proposed potassium channel based mechanism is sufficient to account for the observed propagating pulses of electrical activity, we turned to mathematical modeling. Specifically, we considered a minimal conductance-based toy model describing the dynamics of the cell's membrane potential in terms of a single potassium channel and a leak current (Supplementary Information: Mathematical Model). Consistent with our experimental results, this simple model exhibits transient depolarization followed by hyperpolarization in response to local increases in extracellular potassium concentration (Figure 3d). Furthermore, the model shows long-range propagation of these excitations without decay in the amplitude of membrane potential oscillations (Figure 3e). Therefore, the proposed mechanism is mathematically sufficient to qualitatively account for the observed membrane potential dynamics and active propagation in space.

The model also predicts that reduced efficiency of the potassium channel function could lead to degradation in long-range communication (Figure 3e). Since a complete *yugO* deletion interferes with development of large biofilms[32], we constructed a strain in which we deleted the TrkA gating domain, leaving only the ion channel portion of YugO intact (Supplementary Information: Strains). Similarly truncated bacterial potassium channels have been shown to have altered gating and ion conductance[33,37]. Indeed, the *yugOΔtrkA* mutant biofilms exhibited a reduced propagation of membrane potential oscillations (Figure 3f and Supplementary Video 3). Specifically, in contrast to wild-type, the *yugOΔtrkA* mutant shows decay in the signal amplitude from the interior of the biofilm to the cells at the periphery, which is also consistent with model predictions (Figure 3g). Thus, YugO channel gating appears to promote efficient electrical communication between distant cells.

Discussion

Our findings suggest that bacteria use potassium ion channel mediated electrical signals to coordinate metabolism within the biofilm. The ensuing "bucket brigade" of potassium release allows cells to rapidly communicate their metabolic state, taking advantage of a link between membrane potential and metabolic activity. This form of electrical communication can thus enhance the previously described long-range metabolic codependence in biofilms[17]. Specifically, the wave of depolarization triggered by metabolically stressed interior cells would limit the ability of cells in the biofilm periphery to take up glutamate or retain ammonium, thereby allowing interior cells more access to these nutrients. This also provides a possible explanation for the observation that the *yugO* deletion strain has a defect in biofilm development[32]. Interestingly, owing to the rapid diffusivity of potassium ions in aqueous environments, it is also conceivable that even physically disconnected biofilms could be capable of synchronizing their metabolic oscillations by a similar exchange of potassium ions.

The role of ion channel mediated electrical communication has long been appreciated[38]. While cation channels are found in all organisms[8,9] and potassium is the dominant intracellular cation[24], electrical signaling is commonly viewed to be a property of neurons. However, several recent studies have suggested that in addition to traditional cell-to-cell communication systems such as quorum sensing[39], bacteria may use electron flux[40–42] to communicate. The here described study of electrical coordination of metabolism in microbial communities may in turn hold some general insights that extend beyond bacteria. For example, the connection between neuronal signaling and metabolic activity (neurometabolism) is an active area of research[43,44]. Furthermore, depletion of glutamate, the most common excitatory neurotransmitter[45], also forms the initial trigger for these collective metabolic oscillations synchronized by potassium. Therefore, it is intriguing to think not only about

the structural similarities between bacterial and human potassium ion channels[1,2], but also their possible functional similarities with respect to long-range electrical communication.

Methods

Strains. All experiments were done using *Bacillus subtilis* NCIB 3610. The wild type strain was a gift from Wade Winkler (University of Maryland)[46], and all other strains were derived from it and are listed in Extended Data Figure 5. To make deletion strains, we used polymerase chain reaction (PCR) to amplify the desired regions from the wild type strain. The PCR products were then put within the pER449 vector (gift from Wade Winkler). For the *trkA* mutant, we deleted the C-terminal portion of *yugO* (AA's 117-328), leaving only the N-terminal ion channel portion of *yugO* (AA's 1-116). We identified the *trkA* region using Pfam (http://pfam.xfam.org/). All constructs were confirmed by direct sequencing and then integrated into the chromosome of the wild type strain by a standard one-step transformation procedure[47]. Finally, chromosomal integrations were confirmed by colony PCR using the corresponding primers.

Growth conditions. The biofilms were grown in MSgg medium[16] which contains 5 mM potassium phosphate buffer (pH 7.0), 100 mM MOPS buffer (pH 7.0, adjusted using NaOH), 2 mM $MgCl_2$, 700 μM $CaCl_2$, 50 μM $MnCl_2$, 100 μM $FeCl_3$, 1 μM $ZnCl_2$, 2 μM thiamine HCl, 0.5% (v/v) glycerol and 0.5% (w/v) monosodium glutamate. The MSgg medium was made from stock solutions on the day of the experiment, and the stock solution for glutamate was made new weekly.

Microfluidics. We followed methods similar to a previous study[17]. Briefly, we used the CellASIC ONIX Microfluidic Platform and the Y04D microfluidic plate (EMD Millipore). We used a pump pressure of 1 psi with only one media inlet open, which corresponds to a flow speed of ~16 μm/s. On the day before the experiment, cells from −80°C glycerol stock were streaked onto an LB agar plate and incubated at 37°C overnight. The next morning, a single colony was picked from the plate and inoculated into 3 ml of LB broth and incubated in a 37°C shaker. After 2.5 hours of incubation, the cell culture was centrifuged at 2100 rcf for 1 min, and the cell pellet

was re-suspended in MSgg and immediately loaded into microfluidics. After loading, cells in the microfluidic chamber were incubated at 37°C for 90 min, and then the temperature was kept at 30°C for the rest of the experiment.

Time-Lapse Microscopy. The growth of the biofilms was recorded using phase contrast microscopy. The microscopes used were Olympus IX83 and DeltaVision PersonalDV. To image entire biofilms, 10X objectives were used in most of the experiments. Biofilm phase contrast and fluorescence images were taken every 10 min, except in Figure 2g where images were taken every 5 min. To generate Figure 3b and Extended Data Figures 4a-c, where high temporal resolution was required, images were taken every minute. Whenever fluorescence images were recorded, we used the minimum exposure time that still provided a good signal-to-noise ratio (for example, we typically used 20 ms exposure for ThT and 100 ms exposure for APG-4).

Image analysis. Fiji/ImageJ (National Institutes of Health) and MATLAB (MathWorks) were used for image analysis. We generated custom scripts and used the image analysis toolbox to perform image segmentation on biofilm phase contrast images. To measure biofilm growth rate, we identified the biofilm area in each frame by segmenting the images and took the derivative of biofilm radius over time. We identified the radius by assuming circular growth of the colony and taking the length from the center of the cell trap to the biofilm edge. To generate membrane potential curves, we measured the fluorescence of ThT within the biofilm using the ImageJ "Plot Z-axis Profile" command and performed subsequent analysis, such as normalization and subtracting of baseline signal, in MATLAB.

Experimental reproducibility. Data shown in the main figures were drawn from a minimum of 3 independent experiments and often many more. For example, we analyzed ThT oscillations (represented in Figure 1c-e) in over 75 biofilms. In cases where only a single representative trace is shown, we analyzed multiple regions within the biofilm to ensure accuracy of the analysis. In experiments comparing wild-type and a mutant strain (*yugO* or *yugOΔtrkA)*, we always performed head-to-head experiments (separate chambers in the same microfluidic device) on the same day using the same media to eliminate possible artifacts.

Theoretical estimate of potassium diffusion within biofilms. We used the diffusion coefficient of potassium in water (19.7×10^{-6} cm^2/s)[48] and reduced it to 70% in accordance with a reference on diffusion in biofilms[49], yielding the value of the diffusion coefficient (13.8×10^{-6} cm^2/s) used in the mathematical model as well as the theoretical curves plotted alongside our experimental data. To estimate the rate of potassium propagation by diffusion, we used the formula for 2D mean squared displacement (MSD):

$$r = \sqrt{4Dt}$$

Where r is the displacement, D is the diffusion coefficient, and t is time. We used this relationship to generate the curve shown in Extended Data Figure 3d. We directly compared the log-log slope of the experimental data (slope = 1.1, R^2 = 0.96) to that expected for diffusion (slope = 0.5) to further confirm that the experimental data cannot be explained by simple diffusion.

To estimate the decay of amplitude by diffusion, we used the formula for the concentration profile of 2D diffusion:

$$C(r,t) = \frac{M}{4\pi Dt}\exp\left(-\frac{r^2}{4Dt}\right)$$

Where C is the concentration of potassium at displacement r and time t, M is a constant related to the initial pulse amplitude of potassium that we matched to the initial experimental pulse amplitude of APG-4, and D is the diffusion coefficient. We used this relationship to generate the curve in Figure 2h.

Dyes and Concentrations. Thioflavin T (ThT) and $DiSC_3(5)$ were used at 10 μM. We used ThT and $DiSC_3(5)$ to track relative changes in the membrane potential, where the fluorescence of ThT increases when the cell becomes more inside negative (hyperpolarizes). We found the sensitivity of ThT to be significantly higher than that of $DiSC_3(5)$, where sensitivity is defined as the ratio between the amplitude of oscillation and its error (Extended Data Figure 1a). Furthermore, under our experimental conditions, $DiSC_3(5)$ appears to be absorbed by the PDMS in the microfluidic device. This hinders quantitative analysis (lower sensitivity) and also greatly increases the time required for the dye to diffuse into the biofilm.

APG-4 (TEFLabs) was used at 2 μM. We used the membrane impermeable TMA^+ salt form to track the extracellular concentration of potassium. We verified that APG-4 does not significantly diffuse into cells (Extended Data Figure 2a). We also verified that APG-4 could measure extracellular potassium in MSgg media within our microfluidic device (Extended Data Figure 2b).

We used ANG-2 (TEFLabs) at 2 μM. We used the membrane impermeable TMA^+ salt form to track the extracellular concentration of sodium (Extended Data Figure 3c, d).

End notes

Supplementary Information is linked to the online version of the paper at www.nature.com/nature.

Acknowledgements We would like to thank Steve Lockless, Katherine Süel, Roy Wollman, Tolga Çağatay, and Michael Elowitz for comments during the writing of the manuscript and Christopher Piggott for cloning help. A.P. is a Simons Foundation Fellow of the Helen Hay Whitney Foundation. J.G.O. is supported by the Ministerio de Economia y Competitividad (Spain) and FEDER, under project FIS2012-37655-C02-01, and by the ICREA Academia Programme. This research was funded by the National Institutes of Health, National Institute of General Medical Sciences Grant R01 GM088428 and the National Science Foundation Grant MCB-1450867 50867 (both to G.M.S.). This work was also supported by the San Diego Center for Systems Biology (NIH Grant P50 GM085764).

Author Contributions G.M.S., A.P., J.L., M.A., and J.G.O. designed the research, A.P. and J.L. performed the experiments, J.L. and A.P. performed the data analysis, J.G.O. performed the mathematical

modeling, S.L. made the bacteria strains, G.M.S., A.P., J.L., and J.G.O. wrote the manuscript. All authors discussed the manuscript.

Author Information Reprints and permissions information is available at www.nature.com/reprints. The authors declare no competing financial interest. Correspondence and requests for materials should be addressed to G.M.S. (gsuel@ucsd.edu).

References

1. Hille, B. *Ion Channels of Excitable Membranes*. (2001).

2. MacKinnon, R. Potassium channels and the atomic basis of selective ion conduction. in *Bioscience Reports* **24,** 75–100 (2004).

3. Doyle, D. A. *et al.* The structure of the potassium channel: molecular basis of K+ conduction and selectivity. *Science* **280,** 69–77 (1998).

4. Ren, D. *et al.* A prokaryotic voltage-gated sodium channel. *Science* **294,** 2372–2375 (2001).

5. Iyer, R., Iverson, T. M., Accardi, A. & Miller, C. A biological role for prokaryotic ClC chloride channels. *Nature* **419,** 715–718 (2002).

6. Jiang, Y. *et al.* Crystal structure and mechanism of a calcium-gated potassium channel. *Nature* **417,** 515–522 (2002).

7. Chen, G. Q., Cui, C., Mayer, M. L. & Gouaux, E. Functional characterization of a potassium-selective prokaryotic glutamate receptor. *Nature* **402,** 817–821 (1999).

8. Kuo, M. M. C., Haynes, W. J., Loukin, S. H., Kung, C. & Saimi, Y. Prokaryotic K+ channels: From crystal structures to diversity. *FEMS Microbiology Reviews* **29,** 961–985 (2005).

9. Saimi, Y., Loukin, S. H., Zhou, X. L., Martinac, B. & Kung, C. Ion channels in microbes. *Methods Enzymol.* **294,** 507–524 (1998).

10. Martinac, B., Buechner, M., Delcour, A. H., Adler, J. & Kung, C. Pressure-sensitive ion channel in Escherichia coli. *Proc. Natl. Acad. Sci. U. S. A.* **84,** 2297–2301 (1987).

11. Costerton, J. W., Stewart, P. S. & Greenberg, E. P. Bacterial biofilms: a common cause of persistent infections. *Science* **284,** 1318–1322 (1999).

12. Hall-Stoodley, L., Costerton, J. W. & Stoodley, P. Bacterial biofilms: from the natural environment to infectious diseases. *Nat. Rev. Microbiol.* **2,** 95–108 (2004).

13. Vlamakis, H., Aguilar, C., Losick, R. & Kolter, R. Control of cell fate by the formation of an architecturally complex bacterial community. *Genes Dev.* **22,** 945–953 (2008).

14. Asally, M. *et al.* Localized cell death focuses mechanical forces during 3D patterning in a biofilm. *Proc. Natl. Acad. Sci. U. S. A.* (2012). doi:10.1073/pnas.1212429109

15. Wilking, J. N. *et al.* Liquid transport facilitated by channels in Bacillus subtilis biofilms. *Proc. Natl. Acad. Sci. U. S. A.* **110,** 848–52 (2013).

16. Payne, S. *et al.* Temporal control of self-organized pattern formation without morphogen gradients in bacteria. *Mol. Syst. Biol.* **9,** (2013).

17. Liu, J. *et al.* Metabolic codependence gives rise to collective oscillations within microbial communities. *Nature* **523,** (2015).

18. Tolner, B., Ubbink-Kok, T., Poolman, B. & Konings, W. N. Characterization of the proton/glutamate symport protein of Bacillus subtilis and its functional expression in Escherichia coli. *J. Bacteriol.* **177,** 2863–2869 (1995).

19. Boogerd, F. C. *et al.* AmtB-mediated NH3 transport in prokaryotes must be active and as a consequence regulation of transport by GlnK is mandatory to limit futile cycling of NH4 +/NH3. *FEBS Lett.* **585,** 23–28 (2011).

20. Kralj, J. M., Hochbaum, D. R., Douglass, A. D. & Cohen, A. E. Electrical spiking in Escherichia coli probed with a fluorescent voltage-indicating protein. *Science* **333,** 345–8 (2011).

21. Lo, C.-J., Leake, M. C., Pilizota, T. & Berry, R. M. Nonequivalence of membrane voltage and ion-gradient as driving forces for the bacterial flagellar motor at low load. *Biophys. J.* **93,** 294–302 (2007).

22. Strahl, H. & Hamoen, L. W. Membrane potential is important for bacterial cell division. *Proc. Natl. Acad. Sci. U. S. A.* **107,** 12281–6 (2010).

23. Krulwich, T. A., Sachs, G. & Padan, E. Molecular aspects of bacterial pH sensing and homeostasis. *Nat. Rev. Microbiol.* **9,** 330–343 (2011).

24. Epstein, W. The Roles and Regulation of Potassium in Bacteria. *Progress in Nucleic Acid Research and Molecular Biology* **75,** 293–320 (2003).

25. López, D., Fischbach, M. a, Chu, F., Losick, R. & Kolter, R. Structurally diverse natural products that cause potassium leakage trigger multicellularity in Bacillus subtilis. *Proc. Natl. Acad. Sci. U. S. A.* **106,** 280–5 (2009).

26. Kinsinger, R. F., Kearns, D. B., Hale, M. & Fall, R. Genetic requirements for potassium ion-dependent colony spreading in Bacillus subtilis. *J. Bacteriol.* **187,** 8462–8469 (2005).

27. Vieira-Pires, R. S., Szollosi, A. & Morais-Cabral, J. H. The structure of the KtrAB potassium transporter. *Nature* **496,** 323–8 (2013).

28. Holtmann, G., Bakker, E. P., Uozumi, N. & Bremer, E. KtrAB and KtrCD: Two K+ uptake systems in Bacillus subtilis and their role in adaptation to hypertonicity. *J. Bacteriol.* **185,** 1289–1298 (2003).

29. Whatmore, a M., Chudek, J. a & Reed, R. H. The effects of osmotic upshock on the intracellular solute pools of Bacillus subtilis. *J. Gen. Microbiol.* **136,** 2527–35 (1990).

30. Rimmele, T. S. & Chatton, J. Y. A Novel Optical Intracellular Imaging Approach for Potassium Dynamics in Astrocytes. *PLoS One* (2014).

31. Margolin, Y. & Eisenbach, M. Voltage clamp effects on bacterial chemotaxis. *J. Bacteriol.* **159,** 605–610 (1984).

32. Lundberg, M. E., Becker, E. C. & Choe, S. MstX and a putative potassium channel facilitate biofilm formation in Bacillus subtilis. *PLoS One* **8,** e60993 (2013).

33. Cao, Y. *et al.* Gating of the TrkH ion channel by its associated RCK protein TrkA. *Nature* **496,** 317–22 (2013).

34. Roosild, T. P., Miller, S., Booth, I. R. & Choe, S. A mechanism of regulating transmembrane potassium flux through a ligand-mediated conformational switch. *Cell* **109,** 781–791 (2002).

35. Schlosser, A., Hamann, A., Bossemeyer, D., Schneider, E. & Bakker, E. P. NAD+ binding to the Escherichia coli K+-uptake protein TrkA and sequence similarity between TrkA and domains of a family of dehydrogenases suggest a role for NAD+ in bacterial transport. *Mol. Microbiol.* **9,** (1993).

36. Fisher, S. H. Regulation of nitrogen metabolism in Bacillus subtilis: vive la différence! *Mol. Microbiol.* **32,** 223–32 (1999).

37. Cortes, D. M., Cuello, L. G. & Perozo, E. Molecular architecture of full-length KcsA: role of cytoplasmic domains in ion permeation and activation gating. *J. Gen. Physiol.* **117,** 165–180 (2001).

38. Hodgkin, A. L. & Huxley, A. F. A quantitative description of membrane current and its applications to conduction and excitation in nerve. *J. Physiol.* **117,** 500–544 (1952).

39. Waters, C. M. & Bassler, B. L. Quorum sensing: cell-to-cell communication in bacteria. *Annu. Rev. Cell Dev. Biol.* **21,** 319–346 (2005).

40. Kato, S., Hashimoto, K. & Watanabe, K. Iron-Oxide Minerals Affect Extracellular Electron-Transfer Paths of Geobacter spp. *Microbes Environ.* **28,** 141–148 (2013).

41. Pfeffer, C. *et al.* Filamentous bacteria transport electrons over centimetre distances. *Nature* (2012). doi:10.1038/nature11586

42. Masi, E. *et al.* Electrical spiking in bacterial biofilms. *J R Soc Interface* (2014).

43. Pan, J. W. *et al.* Neurometabolism in human epilepsy. in *Epilepsia* **49,** 31–41 (2008).

44. Petroff, O. A. C., Errante, L. D., Rothman, D. L., Kim, J. H. & Spencer, D. D. Glutamate-glutamine cycling in the epileptic human hippocampus. *Epilepsia* **43,** 703–710 (2002).

45. Meldrum, B. S. Glutamate as a neurotransmitter in the brain: review of physiology and pathology. *J. Nutr.* **130,** 1007S–15S (2000).

46. Irnov, I. & Winkler, W. C. A regulatory RNA required for antitermination of biofilm and capsular polysaccharide operons in Bacillales. *Mol. Microbiol.* **76,** 559–575 (2010).

47. Jarmer, H., Berka, R., Knudsen, S. & Saxild, H. H. Transcriptome analysis documents induced competence of Bacillus subtilis during nitrogen limiting conditions. *FEMS Microbiol. Lett.* **206,** 197–200 (2002).

48. Horvath, A. L. *Handbook of aqueous electrolyte solutions: physical properties, estimation and correlation methods*. (1986).

49. Stewart, P. S. Diffusion in biofilms. *Journal of Bacteriology* **185,** 1485–1491 (2003).

Figure Legends

Figure 1. Biofilms produce synchronized oscillations in membrane potential. *(a)* Biofilms generate collective metabolic oscillations resulting from long-range metabolic interactions between interior and peripheral cells[17]. It remains unclear how microscopic bacteria are capable of communicating over such macroscopic distances within biofilm communities. *(b)* Schematic of the microfluidic device used throughout this study (left). Phase contrast image of a biofilm growing in the microfluidic device with the cell trap highlighted in yellow (right). Scale bar indicates 100 μm. *(c)* Global oscillations in membrane potential, as reported by Thioflavin T (ThT), within the biofilm community. ThT is positively charged but not known to be actively transported, so it can be retained in cells due to their inside-negative membrane potential. ThT fluorescence increases when the inside of the cell becomes more negative, and thus ThT is inversely related to the membrane potential. Scale bar indicates 0.15

mm. Representative images shown are drawn from over 75 independent biofilms. *(d)* Membrane potential oscillations are highly synchronized even between the most distant regions of the biofilm. To analyze synchronization, the edge region of the biofilm was identified and straightened (left) then plotted over time (right). *(e)* Time traces of the heatmap shown in d. Indicated in bold is the mean of 30 traces.

Figure 2. Potassium release is involved in active signal propagation within the biofilm. *(a)* An extracellular fluorescent chemical dye (APG-4) reports the concentration of potassium in the media (Extended Data Figure 2a,b). For comparison, the same cells are shown stained with ThT, which is inversely related to the membrane potential. These images depict cells at the peak of the ThT oscillation cycle. Representative images are selected from 6 independent experiments. Scale bar indicates 2 μm. *(b)* Global oscillations in extracellular potassium throughout the biofilm. A white line indicates the edge of the biofilm. Representative images are selected from 6 independent experiments. Scale bar indicates 0.2 mm. *(c)* Oscillations in membrane potential and extracellular potassium are synchronized, suggesting that potassium release is involved in global membrane potential oscillations. ThT is inversely related to the membrane potential. Representative traces are taken from the experiment shown in b. *(d)* A chemical potassium clamp (300 mM KCl, matching the intracellular concentration[28]) prevents the formation of potassium electrochemical gradients across the cellular membrane. *(e)* Clamping net potassium flux quenches oscillations in membrane potential. Representative trace is selected from 3 independent experiments. *(f)* Illustration of the differences between passive signaling (diffusion) and active signaling. When cells passively respond to a signal, the range that the signal can propagate is limited due to the decay of signal amplitude. In contrast, when cells actively respond by amplifying the signal, propagation can extend over greater distances. *(g)* We measured propagation of extracellular potassium by measuring APG-4 in time and along a

length of approximately 1.5 mm within the biofilm. *(h)* Extracellular potassium amplitude is relatively constant as the signal propagates, in contrast to the predicted amplitude decay of a passive signal. Representative data selected from 6 independent experiments. The diffusion line is calculated using the 2D diffusion equation and the diffusion coefficient for potassium within biofilms (Supplementary Information).

Figure 3. The molecular mechanism of signal propagation involves potassium channel gating. *(a)* *yugO* is a potassium channel in *B. subtilis* that is gated intracellularly by a *trkA* domain, which is regulated by the metabolic state of the cell[33–35]. Withdrawing glutamate (the sole nitrogen source in MSgg media) induces an increase in extracellular potassium (APG-4) for wild-type but not the *yugO* deletion strain. Error bars indicate the mean +/- std for 3 independent biofilms each. *(b)* An external potassium shock (300 mM KCl) induces a short-term membrane potential depolarization in both wild-type and *yugO* deletion strains. However, in the wild-type this initial depolarization was followed by hyperpolarization, which is not observed in the *yugO* deletion strain (mean +/- std for 12 traces drawn from 3 biofilms each). ThT is inversely related to the membrane potential. *(c)* Proposed toy model for potassium signaling. The initial trigger for potassium release is metabolic stress caused by glutamate limitation. External potassium depolarizes neighboring cells, producing further nitrogen limitation by limiting glutamate uptake, and thus produces further metabolic stress. This cycle results in cell-cell propagation of the potassium signal. *(d)* A minimal conductance-based model describing the dynamics of the cell's membrane potential in terms of a single potassium channel and a leak current. Consistent with our experimental results, this simple model exhibits transient depolarization followed by hyperpolarization in response to local increases in extracellular potassium concentration. *(e)* The model predicts that manipulating channel gating and conductance will result in decaying amplitude in the spatial propagation of membrane potential oscillations. *(f)* Maximum intensity projection of

membrane potential change illustrating attenuated communication within the biofilm in a *yugOΔtrkA* deletion compared to wild type biofilms (top). Heatmap of oscillations taken from wild type and *yugOΔtrkA mutant* biofilms (bottom). Representative images are taken from 3 independent experiments in which WT and *yugOΔtrkA* biofilms are compared head-to-head. Scale bars indicate 8 μm. *(g)* Quantification of normalized pulse amplitude from wild type (n = 8 pulses) and *yugOΔtrkA* (n = 12 pulses) mutant biofilms (mean +/- sem).

Extended Data Legends

Extended Data Figure 1. Thioflavin T (ThT) is a fluorescent reporter that is inversely related to the membrane potential. *(a)* ThT and $DiSC_3(5)$, an established reporter of membrane potential in bacteria[22], both oscillate within biofilms. ThT has an approximately three fold higher sensitivity to changes in membrane potential compared to $DiSC_3(5)$. Sensitivity is defined as the ratio between peak height and error in peak height. Error bars indicate mean +/- std (n = 8). *(b)* The cellular ThT fluorescence depends on the external pH, where higher pH results in greater membrane potential as expected[23]. ThT itself is insensitive to these pH changes and the traces are background subtracted to eliminate possible artifacts. Representative trace is selected from 3 independent biofilms. *(c)* Oscillations in ThT and growth rate are inversely correlated, linking membrane potential oscillations to the metabolic cycle which produces periodic growth pauses[17]. Growth rate is calculated by taking the derivative of biofilm radius over time (Supplementary Information). Representative trace is selected from over 75 independent biofilms. *(d)* Replacing glutamate with 0.2% glutamine, which eliminates the need to take up glutamate or retain ammonium, quenches ThT oscillations. This further suggests that ThT oscillations are specific to the metabolic cycle involving glutamate and ammonium. Representative trace is selected from 3 independent experiments.

Extended Data Figure 2. A fluorescent reporter of extracellular potassium (APG-4) indicates that potassium plays a role in membrane potential oscillations. (a) High-resolution images showing the intracellular localization of ThT and primarily extracellular localization of APG-4 (left). Quantification of ThT and APG-4 along the 2μm profile indicated in the phase image indicates that APG-4 does not significantly diffuse into the cell (right). Representative images are selected from 6 independent experiments. *(b)* Induction curve for APG-4 generated using externally supplemented KCl. The experiment was repeated twice. *(c)* Oscillations in extracellular potassium in the surrounding cell-free region during biofilm oscillations. These oscillations occurred during the experiment shown in Figure 2bc and the pulses are synchronized between the biofilm and the surrounding cell-free region. Representative trace is selected from 6 independent experiments. (d) Induction curve for ANG-2 generated using externally supplemented NaCl. Experiment was repeated twice. (e) Simultaneous measurement of ThT and ANG-2 indicates a lack of oscillations in extracellular sodium. Representative trace selected from 3 independent biofilms. (f) Furthermore, perturbing extracellular sodium concentrations in the media had no detectable effect on membrane potential oscillations. Representative trace is selected from 4 independent experiments.

Extended Data Figure 3. *(a)* A chemical potassium clamp (300 mM KCl, matching the intracellular concentration[28], and 30 μM valinomycin) prevents the formation of potassium electrochemical gradients across the cellular membrane. Valinomycin is an antibiotic that creates potassium-specific carriers in the cellular membrane[31]. *(b)* Clamping net potassium flux quenches oscillations in membrane potential. *(c)* Propagation of extracellular potassium is estimated by tracking the half-maximal position of the pulse over time. Representative traces are shown for a single pulse selected from one of 6 independent experiments. *(d)* Propagation of extracellular potassium is relatively

constant over time in contrast to diffusion that is expected to decay. The diffusion line is calculated using the mean squared displacement (MSD) and the diffusion coefficient for potassium in biofilms (Supplementary Information). Slopes are calculated from the same representative data shown in c.

Extended Data Figure 4. External potassium affects the metabolic state of the cell. *(a)* A potassium shock (300 mM KCl) produces an initial ThT decrease (depolarization) followed by a sustained ThT increases (hyperpolarization). ThT is inversely related to the membrane potential. A corresponding pulse in APG-4 during this ThT increase suggests that hyperpolarization is due to release of potassium. APG-4 signal due to the external potassium shock itself was subtracted using the cell-free background near the biofilm. Representative trace is selected from 3 independent experiments. *(b)* ThT spikes in response to external potassium shock (300 mM KCl) but not an equivalent shock of 300 mM sorbitol, an uncharged solute. Representative trace is selected from 3 independent experiments. *(c)* The hyperpolarization response occurs when cells are grown in glutamate but not when glutamate is replaced by 0.2% glutamine, which bypasses the need to take up glutamate or retain ammonium. Representative trace is selected from 4 independent biofilms.

Extended Data Figure 5. List of strains used in this study.

Extended Data Figure 6. Parameter values used in the model.

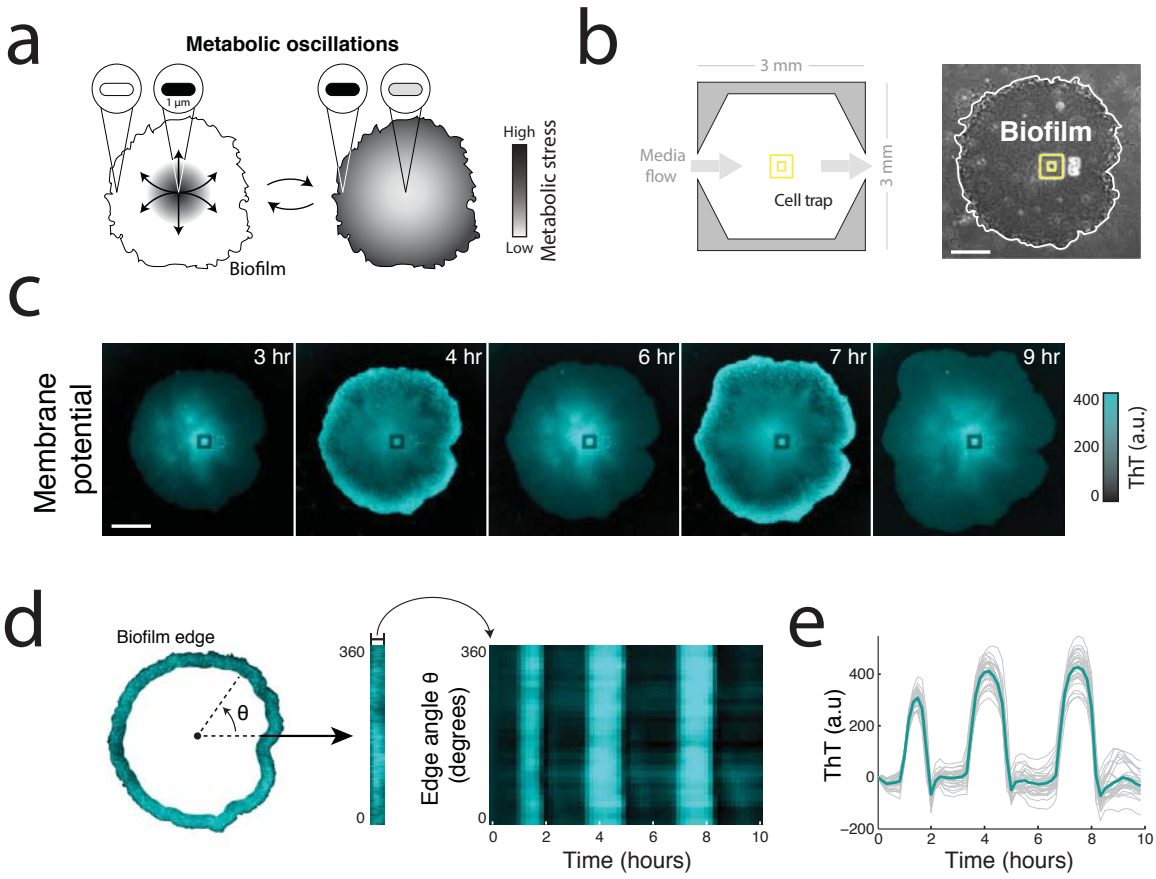

Figure 1: Prindle et al.

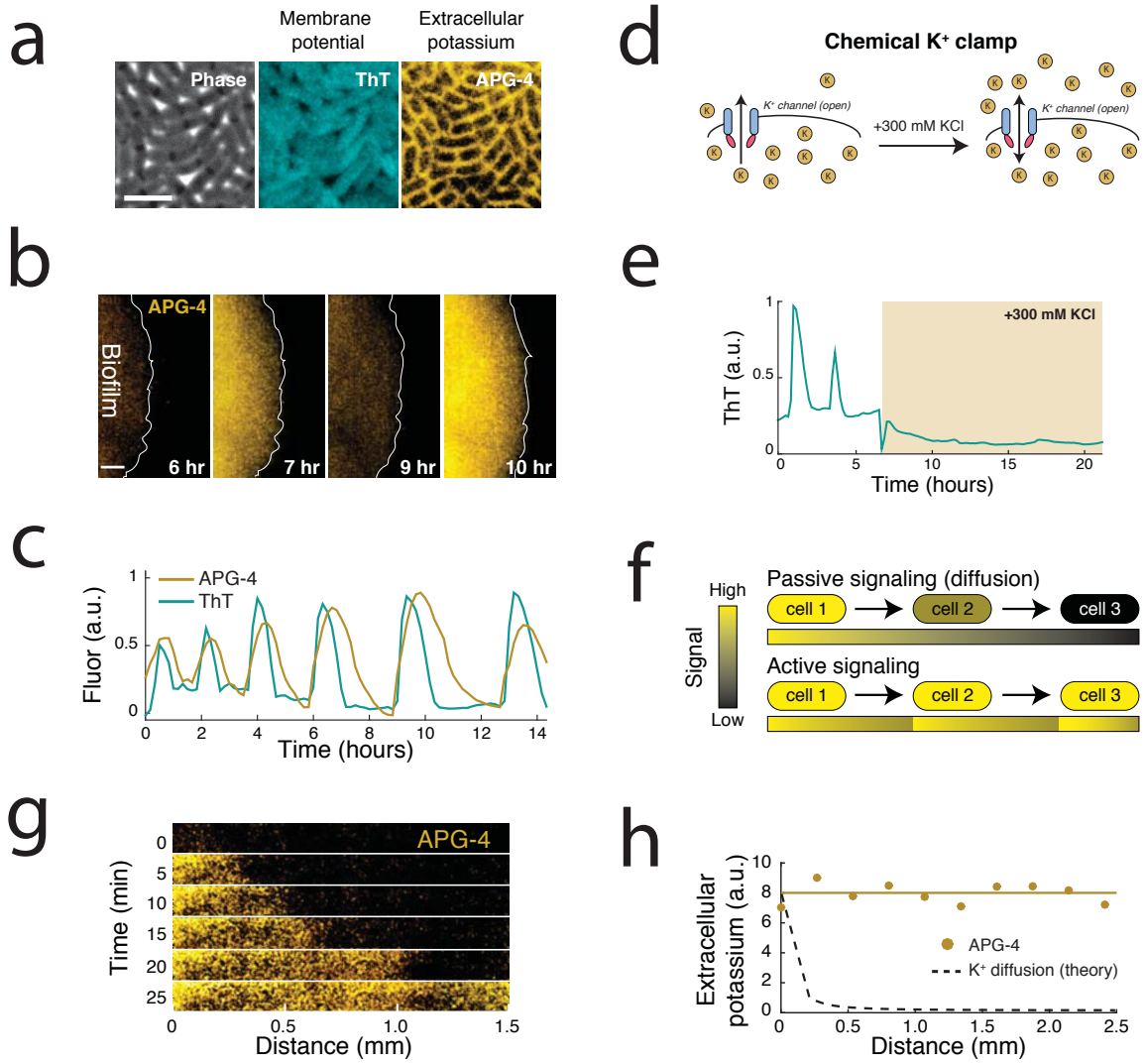

Figure 2: Prindle et al.

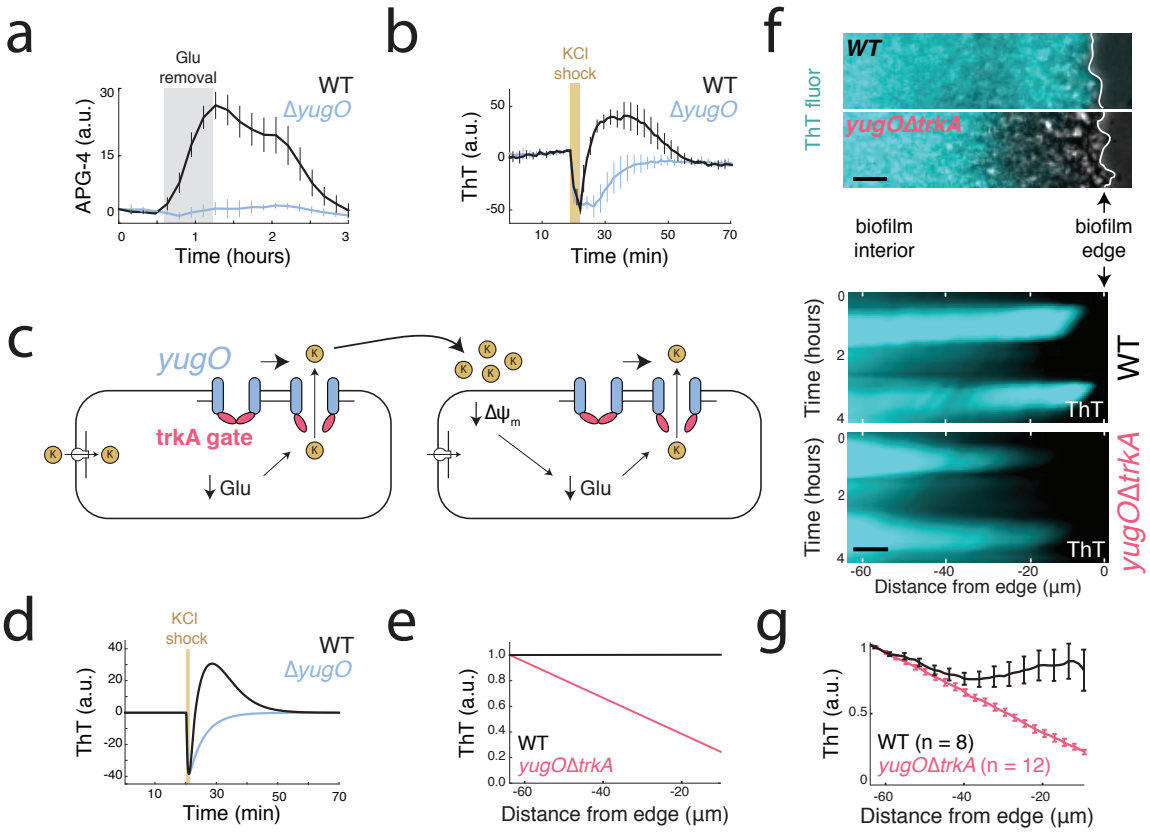

Figure 3: Prindle et al.